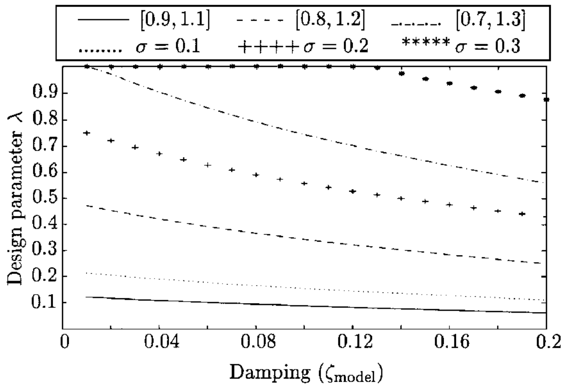

Fig. 6 Optimal design parameters for hybrid shapers under uniform and Gaussian uncertainty in frequency.

As shown in Fig. 6, for $\sigma = 0.3$ and low damping ($\zeta_{\text{model}} < 0.13$), the design parameter is fixed at the value $\lambda = 1$. It is possible to have $\lambda > 1$, but this will cause the second amplitude A_2 to be negative and we were interested in positive amplitude shapers [see Eq. (2)]. This suggests that, when uncertainties are very large (and ζ_{model} is small), the best designs or more appropriate designs are those obtained by taking convex combinations of ZVDD and 2-hump EI shapers.

Conclusions

The expected residual vibration performance measure easily incorporates the probability distribution of modeling errors in both natural frequencies and damping coefficients. Using this new measure to analyze several traditional input shaping designs shows that the EI and multihump shapers yield lower expected residual vibration than the equivalent length ZVD and derivative-type shapers for large uncertainties in the natural frequency or large uncertainties in both natural frequency and damping constant. However, the ZVD and derivative shapers lead to smaller residual vibration levels when there is uncertainty in the damping. The results presented also clearly indicate at what uncertainty levels the performance of the EI and multihump shapers become superior to the ZVD and derivative-type shapers, and these results are useful in guiding the choice of the most appropriate type of shaper given the expected variation in the system parameters.

Finally, the proposed hybrid shaper design provides a useful method for deriving shapers that can achieve near-minimal expected residual vibration levels by adjusting only a single design parameter. This method provides a straightforward procedure without resorting to sophisticated numerical optimizers. The simplicity of the hybrid design approach is valuable for an online adaptive controller, whereas the full optimal designs are more feasible in applications requiring only offline computations.

Acknowledgments

The authors gratefully acknowledge support from a National Science Foundation Early Faculty CAREER Award (Grant CMS-9625086), the Colorado Advanced Software Institute, Storage Technology Corporation, and an Office of Naval Research Young Investigator Award (Grant N00014–97–1–0642).

References

[1]Singer, N., and Seering, W., "Preshaping Command Inputs to Reduce System Vibration," *Journal of Dynamic Systems, Measurement and Control*, Vol. 112, No. 1, 1990, pp. 76–82.

[2]Singhose, W. E., Porter, L. J., Tuttle, T. D., and Singer, N. C., "Vibration Reduction Using Multi-Hump Input Shapers," *Journal of Dynamic Systems, Measurement and Control*, Vol. 119, No. 2, 1997, pp. 320–326.

[3]Pao, L. Y., Chang, T. N., and Hou, E., "Input Shaper Designs for Minimizing the Expected Level of Residual Vibration in Flexible Structures," *Proceedings of the American Control Conference* (Albuquerque, NM), Inst. of Electrical and Electronics Engineers, Piscataway, NJ, 1997, pp. 3542–3546.

[4]Pao, L. Y., "Analysis of the Frequency, Damping, and Total Insensitivities of Input Shaping Designs," *Journal of Guidance, Control, and Dynamics*, Vol. 20, No. 5, 1997, pp. 909–915.

Formalized Approach to Obtaining Optimal Coefficients for Coning Algorithms

Chan Gook Park* and Kwang Jin Kim†
Kwangwoon University,
Seoul 139-701, Republic of Korea
and
Jang Gyu Lee‡ and Dohyoung Chung§
Seoul National University,
Seoul 151-742, Republic of Korea

Introduction

Attitude computation has played a key role in strapdown inertial navigation systems because the computed attitude has been continuously used for transforming the vehicle acceleration measured by the accelerometers rigidly attached to the host vehicle. Commonly used attitude updating algorithms for strapdown systems are the Euler method, the direction cosine method, and the quaternion method. Among them, the quaternion method is quite popular due to the advantages of its nonsingularity, simplicity, and computational efficiency.[1] Further improvements on the quaternion method have been made possible by Bortz,[2] Jordan,[3] Miller,[4] Ignagni,[5] Lee et al.,[6] and Jiang[7] using the concepts of rotation vector. It has been proven that the quaternion updating method with the rotation vector can effectively suppress the noncommutativity error,[4–7] which is one of the major error sources in numerical solutions of the attitude equation. The concept for optimizing coning compensation algorithms for strapdown inertial systems was first introduced and applied by Miller.[4] Ignagni[5] showed that, although only pure coning angular rate environment is considered, the algorithm optimization procedure is applicable to generalized vibrational environments.

Recently, Ignagni[8] proposed the concept leading to optimal accuracy characteristics and minimum computational throughput required in a pure coning environment. The algorithms that use the enhancement concept have the simplest form generating many distinct sensor-data cross products and optimal coefficients minimizing the coning compensation error. In this Note, a formalized approach to determining the optimal coefficients in the coning algorithms is proposed. The effectiveness of the proposed approach is demonstrated by applying not only many of the existing coning algorithms but also the determination of the optimal coefficients for six-data-interval case.

Quaternion Update Using the Rotation Vector

The key operation of the attitude algorithm is to properly update the quaternion and rotation vector.[4] The quaternion update $\bar{Q}(t+h)$ is obtained by the following quaternion multiplication:

$$\bar{Q}(t+h) = \bar{Q}(t) * \bar{q}(h) \tag{1}$$

Presented as Paper 96-3736 at the AIAA Guidance, Navigation, and Control Conference, San Diego, CA, July 29–31, 1996; received April 23, 1997; revision received Aug. 27, 1998; accepted for publication Aug. 28, 1998.

*Associate Professor, Department of Control and Instrumentation Engineering.

†Graduate Student, Department of Control and Instrumentation Engineering; currently Researcher, Agency for Defense Development, Daejon 305-600, Republic of Korea.

‡Professor, School of Electrical Engineering and Automatic Control Research Center. Senior Member AIAA.

§Graduate Student, School of Electrical Engineering and Automatic Control Research Center; currently Researcher, Samsung Electronics Co., Ltd., Suwon 442-742, Republic of Korea.

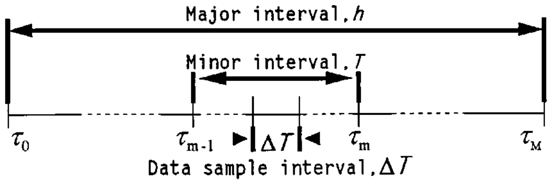

Fig. 1 Intervals associated with coning compensation.

where $*$ indicates quaternion multiplication and $\bar{q}(h)$ is an updating quaternion during the time interval h and is expressed by the usual quaternion relation, namely,

$$\bar{q}(h) = [\cos(\phi_0/2), (\boldsymbol{\phi}/\phi_0)\sin(\phi_0/2)] \tag{2}$$

where $\boldsymbol{\phi}$ represents the rotation vector with the magnitude $\phi_0 = (\boldsymbol{\phi}\cdot\boldsymbol{\phi})^{1/2}$. The rotation vector differential equation for small $\boldsymbol{\phi}$ can be approximated as[2,9]

$$\dot{\boldsymbol{\phi}} = \boldsymbol{\omega} + \tfrac{1}{2}\boldsymbol{\phi}\times\boldsymbol{\omega} + \tfrac{1}{12}\boldsymbol{\phi}\times(\boldsymbol{\phi}\times\boldsymbol{\omega}) \tag{3}$$

where $\boldsymbol{\omega}$ represents the angular rate vector and $\times$ denotes the vector cross product. The last two terms in Eq. (3) are referred to as the noncommutativity rate vector. It must be determined and compensated by gyro measurement to maintain the high accuracy of strapdown attitude algorithms. However, the triple-cross-product term is assumed to be quite small and can be neglected.[4,5]

In the development of the coning compensation algorithm, it is assumed that each major attitude interval is divided into a number of minor intervals, each in turn being divided into a number of data sample intervals over which the gyro incremental angle is measured, as shown in Fig. 1. It presents the most general representation of interval inasmuch as no restriction is placed on the number of sensor data intervals contained in a major attitude update interval. It is desirable to update the rotation vector in every minor interval, whereas the quaternion is updated only once in every major interval.

Formalized Coning Compensation Algorithm

To develop the coning compensation algorithm, it is assumed that the body undergoes pure coning motion, defined by the angular rate vector

$$\boldsymbol{\omega} = a\Omega\cos\Omega\tau\boldsymbol{I} + b\Omega\sin\Omega\tau\boldsymbol{J} \tag{4}$$

where

- $\boldsymbol{\omega}$ = angular rate vector with components expressed in the body frame
- a, b = amplitudes of the angular oscillations in two orthogonal axes of the body
- Ω = frequency associated with the angular oscillations
- $\boldsymbol{I}, \boldsymbol{J}$ = unit vectors along the two body axes about which the oscillations are occurring

The integrated rate vector is determined as

$$\boldsymbol{\alpha}(\tau, \tau_{m-1}) = \int_{\tau_{m-1}}^{\tau} \boldsymbol{\omega}\,\mathrm{d}\tau$$
$$= a(\sin\Omega\tau - \sin\Omega\tau_{m-1})\boldsymbol{I} + b(\cos\Omega\tau_{m-1} - \cos\Omega\tau)\boldsymbol{J} \tag{5}$$

If the angular rate in Eq. (4) is applied to two axes $\boldsymbol{I}$ and $\boldsymbol{J}$, the vehicle goes through the coning motion for $\boldsymbol{K}$ axis. When one period of the coning motion is completed, the drift error, which is the component of the noncommutativity error, is generated in the $\boldsymbol{I}$ and $\boldsymbol{J}$ axes.

Let us define the coning correction over a minor computational interval from τ_{m-1} to τ_m as[10]

$$\delta\boldsymbol{\phi}_m = \frac{1}{2}\int_{\tau_{m-1}}^{\tau_m} \boldsymbol{\alpha}(\tau, \tau_{m-1})\times\boldsymbol{\omega}\,\mathrm{d}\tau \tag{6}$$

The relationship between the rotation vector and the coning correction term will be given in Eq. (18).

Applying the coning motion in Eqs. (4) and (5) to Eq. (6), we obtain

$$\delta\boldsymbol{\phi}_m = (ab\Omega/2)[T - (1/\Omega)\sin\Omega T]\boldsymbol{K} \tag{7}$$

The coning correction given by Eq. (7) reveals an interesting property in that it does not depend on the index m, which designates mth minor interval. Rather, it depends only on the duration of the minor interval T.

For the coning environment defined by Eq. (6), the incremental angular rate over a data sample interval of duration ΔT from t_{k-1} to t_k is

$$\Delta\boldsymbol{\theta}(k) = \boldsymbol{\alpha}(t_k, t_{k-1}) = a(\eta\sin\Omega t_{k-1} + \nu\cos\Omega t_{k-1})\boldsymbol{I}$$
$$+ b(\nu\sin\Omega t_{k-1} - \eta\cos\Omega t_{k-1})\boldsymbol{J} \tag{8}$$

where $\eta = \cos\lambda - 1$, $\nu = \sin\lambda$, and $\lambda = \Omega\Delta T$.

The cross product of two incremental attitude vectors $\Delta\boldsymbol{\theta}(i)\times\Delta\boldsymbol{\theta}(j)$ taken over by different data sample intervals becomes[8]

$$\Delta\boldsymbol{\theta}(i)\times\Delta\boldsymbol{\theta}(j) = ab\{2\sin[(j-i)\lambda]$$
$$- \sin[(j-i+1)\lambda] - \sin[(j-i-1)\lambda]\}\boldsymbol{K} \tag{9}$$

As it can be seen in the coning correction of Eq. (7), the value of the cross product of two attitude increments is independent of the absolute time, but depends only on a multiple of the interval ΔT. Hence, it can be seen that Eq. (7) can be approximated by using Eq. (9).

Lee et al.[6] introduced the concept of distance between the cross products in Eq. (9). It was found that cross products with equal distance behave exactly the same for coning inputs. Taking advantage of this property allows a generalized form for the coning integral algorithm such as[8]

$$\delta\hat{\boldsymbol{\phi}}_m = \left[\sum_{j=n-p+1}^{n} k_{2n-j}\Delta\boldsymbol{\theta}_{m-1}(j) + \sum_{i=1}^{n-1} k_{n-i}\Delta\boldsymbol{\theta}_m(i)\right]\times\Delta\boldsymbol{\theta}_m(n) \tag{10}$$

where n is the number of sample for mth minor interval, p is the number of sample for $(m-1)$th minor interval, $\Delta\boldsymbol{\theta}_m(i)$ is ith gyro sample for mth minor interval, $\Delta\boldsymbol{\theta}_{m-1}(j)$ is jth gyro sample for $(m-1)$th minor interval, and k_{2n-j} and k_{n-i} are the respective constants for distance $2n-j$ and $n-i$ for $\Delta\boldsymbol{\theta}_m(n)$.

Substituting Eq. (9) into Eq. (10), we obtain

$$\delta\hat{\boldsymbol{\phi}}_m = ab[k_{n+p-1}\{2\sin(n+p-1)\lambda - \sin(n+p)\lambda$$
$$- \sin(n+p-2)\lambda\} + \cdots + k_n\{2\sin n\lambda - \sin(n+1)\lambda$$
$$- \sin(n-1)\lambda\} + \cdots + k_1\{2\sin\lambda - \sin 2\lambda - \sin 0\lambda\}]\boldsymbol{K} \tag{11}$$

Expanding each term in Eq. (11) using the Taylor series, the coning correction over the minor interval is obtained as

$$\delta\hat{\boldsymbol{\phi}}_m = ab\Big\{[A_{11}k_1 + A_{12}k_2 + \cdots + A_{1j-1}k_{n+p-2}$$
$$+ A_{1j}k_{n+p-1}]\lambda^3 - [A_{21}k_1 + A_{22}k_2 + \cdots + A_{2j-1}k_{n+p-2}$$
$$+ A_{2j}k_{n+p-1}]\lambda^5 + \cdots + (-1)^{i+1}[A_{i1}k_1 + A_{i2}k_2$$
$$+ \cdots + A_{ij-1}k_{n+p-2} + A_{ij}k_{n+p-1}]\lambda^{2i+1} + \cdots\Big\}\boldsymbol{K} \tag{12}$$

where A_{ij} is a constant defined as

$$A_{ij} = \frac{(j+1)^{2i+1} - 2\cdot j^{2i+1} + (j-1)^{2i+1}}{(2i+1)!} \tag{13}$$

To find k_i $(i = 1, 2, \ldots, n+p-1)$ in Eq. (12), the true coning correction in Eq. (7) is expanded using the Taylor series, and it becomes

$$\delta\boldsymbol{\phi}_m = \frac{ab}{2}\left[\frac{(\Omega T)^3}{3!} - \frac{(\Omega T)^5}{5!} + \cdots\right]\boldsymbol{K}$$
$$= ab\big[c_1\lambda^3 - c_2\lambda^5 + \cdots - (-1)^i c_i\lambda^{(2i+1)} + \cdots\big]\boldsymbol{K} \tag{14}$$

where c_i is defined as

$$c_i = \frac{n^{(2i+1)}}{(2i+1)!\times 2} \tag{15}$$

Suppose that the number of total sample N is $p+n$, then the number of unknown parameters k_i is $N-1$. Using Eqs. (12) and (14), the simultaneous equation for the unknown parameter k_i can be expressed as follows:

$$\underset{(N\times N)}{[A_{ij}]}\ \underset{(N\times 1)}{[k_i]} = \underset{(N\times 1)}{[c_i]} \qquad (i=1,\ldots,N;\quad j=1,\ldots,N) \tag{16}$$

Once n and p are selected, the corresponding optimal coning compensation algorithm can be designed by the following procedure. First, the constants A_{ij} and c_i are calculated from Eqs. (13) and (15), respectively. Second, the unknown coefficient k_i is solved by Eq. (16). Finally, the optimal coning compensation algorithm is obtained by inserting k_i into Eq. (10). Using the formalized procedure, we can easily design optimal coning compensation algorithms for any combinations of n and p.

Furthermore, k_i in Eq. (16) can be simply expressed using a matrix equation. For the case when the number of total sample is less than or equal to seven, the optimal set of coefficients satisfies the following matrix equation:

$$\begin{array}{cccccc} \boldsymbol{N=2} & \boldsymbol{N=3} & \boldsymbol{N=4} & \boldsymbol{N=5} & \boldsymbol{N=6} & \boldsymbol{N=7} \end{array}$$
$$\begin{bmatrix} 1 & 2 & 3 & 4 & 5 & 6 \\ \frac{1}{4} & \frac{3}{2} & \frac{19}{4} & 11 & \frac{85}{4} & \frac{73}{2} \\ \frac{1}{40} & \frac{23}{60} & \frac{289}{120} & \frac{283}{30} & \frac{667}{24} & \frac{4069}{60} \\ \frac{17}{12{,}096} & \frac{311}{6048} & \frac{827}{1344} & \frac{12{,}071}{3024} & \frac{214{,}453}{12{,}096} & \frac{41{,}021}{672} \\ \frac{31}{604{,}800} & \frac{437}{100{,}800} & \frac{58{,}213}{604{,}800} & \frac{153{,}851}{151{,}200} & \frac{816{,}167}{120{,}960} & \frac{9{,}852{,}733}{302{,}400} \\ \frac{1}{760{,}320} & \frac{289}{1{,}140{,}480} & \frac{23{,}417}{228{,}096} & \frac{99{,}641}{570{,}240} & \frac{3{,}914{,}431}{2{,}280{,}960} & \frac{2{,}636{,}935}{228{,}096} \end{bmatrix} \begin{bmatrix} k_1 \\ k_2 \\ k_3 \\ k_4 \\ k_5 \\ k_6 \end{bmatrix} = \begin{bmatrix} \frac{n^3}{12} \\ \frac{n^5}{240} \\ \frac{n^7}{10{,}080} \\ \frac{n^9}{725{,}760} \\ \frac{n^{11}}{79{,}833{,}600} \\ \frac{n^{13}}{12{,}454{,}041{,}600} \end{bmatrix} \tag{17}$$

Hence, k_i can be obtained by matrix inversion and multiplication. After k_i are determined, the optimal coning algorithm can be found by using Eq. (10).

Computed from Eq. (12), $\delta\hat{\boldsymbol{\phi}}_m$ is later used for updating the rotation vector $\boldsymbol{\phi}_m$ over the mth minor interval such as[7,8]

$$\boldsymbol{\phi}_m = \boldsymbol{\phi}_{m-1} + \boldsymbol{\theta}_m + \tfrac{1}{2}\boldsymbol{\phi}_{m-1}\times\boldsymbol{\theta}_m + \delta\hat{\boldsymbol{\phi}}_m \tag{18}$$

where $\boldsymbol{\theta}_m$ is represented by the gyro samples over mth minor interval as follows:

$$\boldsymbol{\theta}_m = \sum_{i=1}^{n}\Delta\boldsymbol{\theta}_m(i) \tag{19}$$

Next the algorithm error is derived to analyze the performance of the optimal coning compensation algorithm. The basic relationships used in deriving the optimal algorithm coefficients can also be employed in establishing the accuracy associated with each algorithm in a pure coning environment. The error ε is defined as the error contained in approximation as follows:

$$\varepsilon = \delta\hat{\boldsymbol{\phi}}_m - \delta\boldsymbol{\phi}_m \tag{20}$$

Substituting Eqs. (12) and (14) into Eq. (20), it is found that the most dominant error in ε is

$$\phi_\varepsilon = \frac{n^{-2(p+n)}\times(p+n)!}{2^{(p+n+1)}\times\prod_{k=1}^{(p+n)+1}(2k-1)}ab(\Omega T)^{2(p+n)+1}\ \text{(rad)} \tag{21}$$

Note that the algorithm error mainly depends on the total number of samples.

Algorithms

It is well known[4,6] that the multiple sample algorithm is superior to the single sample algorithm for high-frequency base motion because the error in updating the rotation vector depends mainly on the number of gyro samples, and many coning compensation algorithms have been previously developed accordingly. In this section, the coning error compensation algorithm and the resulting errors for various number of samples are derived using the proposed procedure.

Each algorithm is obtained, accordingly, from Eqs. (13), (15), (16), and (10). The corresponding error is also obtained from Eq. (21).

Algorithm 1 (Three Samples and One Previous Sample)

When using three present samples and one previous sample, $n=3$, $p=0$, and $N=3$. Using Eq. (17) k_1 and k_2 can be computed. Then, the algorithm becomes

$$\delta\hat{\boldsymbol{\phi}}_m = \left[\frac{3}{280}\Delta\boldsymbol{\theta}_{m-1}(3) + \frac{57}{140}\Delta\boldsymbol{\theta}_m(1) + \frac{393}{280}\Delta\boldsymbol{\theta}_m(2)\right]\times\Delta\boldsymbol{\theta}_m(3) \tag{22}$$

and the error becomes

$$\phi_\varepsilon = \frac{ab}{420}\lambda^9 = \frac{ab}{8{,}266{,}860}(\Omega T)^9 \tag{23}$$

This result is identical to Jiang's result[6] and Ignagni's result.[8]

Algorithm 2 (Four Samples)

In this case $n=4$, $p=0$, and $N=4$, and the algorithm becomes

$$\delta\hat{\boldsymbol{\phi}}_m = \left[\frac{18}{35}\Delta\boldsymbol{\theta}_m(1) + \frac{92}{105}\Delta\boldsymbol{\theta}_m(2) + \frac{214}{105}\Delta\boldsymbol{\theta}_m(2)\right]\times\Delta\boldsymbol{\theta}_m(4) \tag{24}$$

and the error becomes

$$\phi_\varepsilon = \frac{ab}{315}\lambda^9 = \frac{ab}{82{,}575{,}360}(\Omega T)^9 \tag{25}$$

This result is identical to the one presented in Refs. 5 and 8. The resulting error of Eq. (25) has the same power of ΩT as that of Eq. (23). Hence, it can be seen that the magnitude of error depends mainly on the total number of gyro samples rather than on the number of samples in the minor interval.

Algorithm 3 (Five Samples)

The five-sample algorithm has been recently introduced by Ignagni.[8] In this case $n=5$, $p=0$, and $N=5$. Then the algorithm becomes

$$\delta\hat{\boldsymbol{\phi}}_m = \left[\frac{125}{252}\Delta\boldsymbol{\theta}_m(1) + \frac{25}{24}\Delta\boldsymbol{\theta}_m(2) + \frac{325}{252}\Delta\boldsymbol{\theta}_m(3) + \frac{1375}{504}\Delta\boldsymbol{\theta}_m(4)\right]\times\Delta\boldsymbol{\theta}_m(5) \tag{26}$$

and its error becomes

$$\phi_\varepsilon = \frac{5ab}{5544}\lambda^{11} = \frac{ab}{54{,}140{,}625{,}000}(\Omega T)^{11} \tag{27}$$

Algorithm 4 (Six Samples)

The six-sample algorithm has not been previously introduced. However, using the proposed method it can be easily accomplished. In this case $n = 6$, $p = 0$, and $N = 6$, and k_i can be calculated from Eq. (17) as follows:

$$k_1 = \frac{15{,}797}{4620}, \quad k_2 = \frac{3917}{2310}, \quad k_3 = \frac{608}{385}$$
$$k_4 = \frac{2279}{2310}, \quad k_5 = \frac{463}{924} \tag{28}$$

Hence, the algorithm becomes

$$\delta\hat{\phi}_m = [k_5\Delta\boldsymbol{\theta}_m(1) + k_4\Delta\boldsymbol{\theta}_m(2) + k_3\Delta\boldsymbol{\theta}_m(3) + k_2\Delta\boldsymbol{\theta}_m(4) + k_1\Delta\boldsymbol{\theta}_m(5)] \times \Delta\boldsymbol{\theta}_m(6) \tag{29}$$

Its error can also be calculated from Eq. (21), and it becomes

$$\phi_\varepsilon = \frac{ab}{4004}\lambda^{13} = \frac{ab}{52{,}295{,}018{,}840{,}064}(\Omega T)^{13} \tag{30}$$

The error for six-sample algorithm has the 13th power of ΩT, and it concurs with the earlier statement that the magnitude of error depends mainly on the total number of samples.

Conclusion

In this Note, a formalized approach to obtaining optimal coefficients for strapdown coning compensation algorithms is proposed. It is shown by examples that optimal coefficients for the existing attitude algorithms and the six-data interval case can easily be obtained using the proposed approach. The main advantage of using the formalized approach is its easy applications to various combinations of sample numbers. Thus, it enables the attitude algorithm designers to choose the most effective coning compensation algorithm for their attitude computation specifications efficiently.

Acknowledgment

This work was supported by the Special Project Fund given to the Automatic Control Research Center, Seoul National University, by the Agency for Defense Development.

References

[1]Wilcox, J. C., "A New Algorithm for Strapdown Inertial Navigation," *IEEE Transactions on Aerospace and Electronic Systems*, Vol. AES-3, No. 5, 1967, pp. 796–802.

[2]Bortz, J. E., "A New Mathematical Formulation for Strapdown Inertial Navigation," *IEEE Transactions on Aerospace and Electronic Systems*, Vol. AES-7, No. 1, 1971 , pp. 61–66.

[3]Jordan, J. W., "An Accurate Strapdown Direction Cosine Algorithm," NASA TN D-5384, Sept. 1969.

[4]Miller, R. B., "A New Strapdown Attitude Algorithm," *Journal of Guidance, Control, and Dynamics*, Vol. 6, No. 4, 1983, pp. 287–291.

[5]Ignagni, M. B., "Optimal Strapdown Attitude Integration Algorithms," *Journal of Guidance, Control, and Dynamics*, Vol. 13, No. 4, 1990, pp. 738–743.

[6]Lee, J. G., Yoon, Y. J., Mark, J. G., and Tazartes, D. A., "Extension of Strapdown Attitude Algorithm for High-Frequency Base Motion," *Journal of Guidance, Control, and Dynamics*, Vol. 13, No. 4, 1990, pp. 738–743.

[7]Jiang, Y. F., and Lin, Y. P., "Improved Strapdown Coning Algorithms," *IEEE Transactions on Aerospace and Electronic Systems*, Vol. AES-28, No. 2, 1992, pp. 484–490.

[8]Ignagni, M. B., "Efficient Class of Optimal Coning Compensation Algorithms," *Journal of Guidance, Control, and Dynamics*, Vol. 19, No. 2, 1996, pp. 424–429.

[9]Jiang, Y. F., and Lin, Y. P., "On the Rotation Vector Differential Equation," *IEEE Transactions on Aerospace and Electronic Systems*, Vol. AES-27, No. 1, 1991, pp. 181–183.

[10]Savage, P. G., "Strapdown System Algorithms," AGARD-LS-133, 1984, pp. 202–212.

Flutter Boundary Prediction Using Physical Models and Experimental Data

A. Turevskiy,* E. Feron,† and J. Paduano‡
Massachusetts Institute of Technology, Cambridge, Massachusetts 02139

I. Introduction

THE possible occurence of flutter is an important factor that slows down the aircraft flight envelope clearance because it is not very well known in advance and might have catastrophic consequences. Any improvement in predicting the aircraft flutter boundary might, therefore, simultaneously impact the safety and cost of the flight test process.[1]

Several techniques exist to predict flutter boundaries. The first is to track the damping ratios of all flexible modes of the aircraft[2]: Proximity to flutter is declared when one or more damping ratios are approaching zero. Accurate flutter boundary predictions based on this approach require the aircraft to be very close to the actual flutter boundary. This method is nevertheless very popular because it is computationally inexpensive.

Another way to predict the flutter boundary is to develop and use analytical models of aircraft flexible dynamics and unsteady aerodynamic forces. The structural part of the model is obtained from finite element analysis, whereas unsteady aerodynamic forces are approximated using standard linear systems theory.[3,4] In this model, dynamic pressure and Mach numbers are parameters that may be varied until the model dynamics are unstable, thus providing an analytical flutter boundary estimate. From that standpoint, it is similar to the so-called p–k iteration method.[5] This approach provides a priori information about possible flutter mechanisms and flutter boundaries. The quality of the results remains, however, dependent on modeling accuracy.

In this Note, a simple method is developed to update a physical aircraft wing mathematical model with wind-tunnel test data to predict more reliable flutter boundary estimates. The method could potentially apply to full aircraft models and flight test data as well. It uses nonlinear optimization to match the poles of the analytical model to the experimentally identified poles of the aircraft. From that standpoint, the proposed method is similar, but not identical to previous research efforts.[6,7] It is experimentally validated on a wind-tunnel entry.

II. Models and Data for Flutter Boundary Estimation

Analytical Models

A common aircraft aeroelastic model is written in the Laplace transform domain as[4]

$$Ms^2\eta(s) + Cs\eta(s) + K\eta(s) + \bar{q}Q(s)\eta(s) = 0 \tag{1}$$

The first three terms M, C, and K correspond to the system's mass, damping, and stiffness matrices, respectively. The fourth term represents the effect of aerodynamics on the system, and $\bar{q} = \rho V^2/2$ is the dynamic pressure. The effect of unsteady aerodynamics is captured by rational functions of the form

$$Q(s) = A_0 + A_1\bar{s} + A_2\bar{s}^2 + [\bar{s}/(\bar{s}+\beta_1)A_3] + [\bar{s}/(\bar{s}+\beta_2)A_4] \quad \text{with} \quad \bar{s} = (b/V)s$$

Received June 4, 1998; revision received Sept. 5, 1998; accepted for publication Sept. 8, 1998.

*Graduate Research Assistant, Department of Aeronautics and Astronautics, 77 Massachusetts Avenue; currently Engineer, Propulsion Systems Analysis Department, Pratt and Whitney. E-mail: turevska@pweh.com.

†Assistant Professor, Department of Aeronautics and Astronautics, Room 33-217, 77 Massachusetts Avenue. E-mail: feron@mit.edu. Senior Member AIAA.

‡Associate Professor, Department of Aeronautics and Astronautics, Room 33-103, 77 Massachusetts Avenue. E-mail: jdpaduan@mit.edu. Member AIAA.